Supplemental Figures and Legends

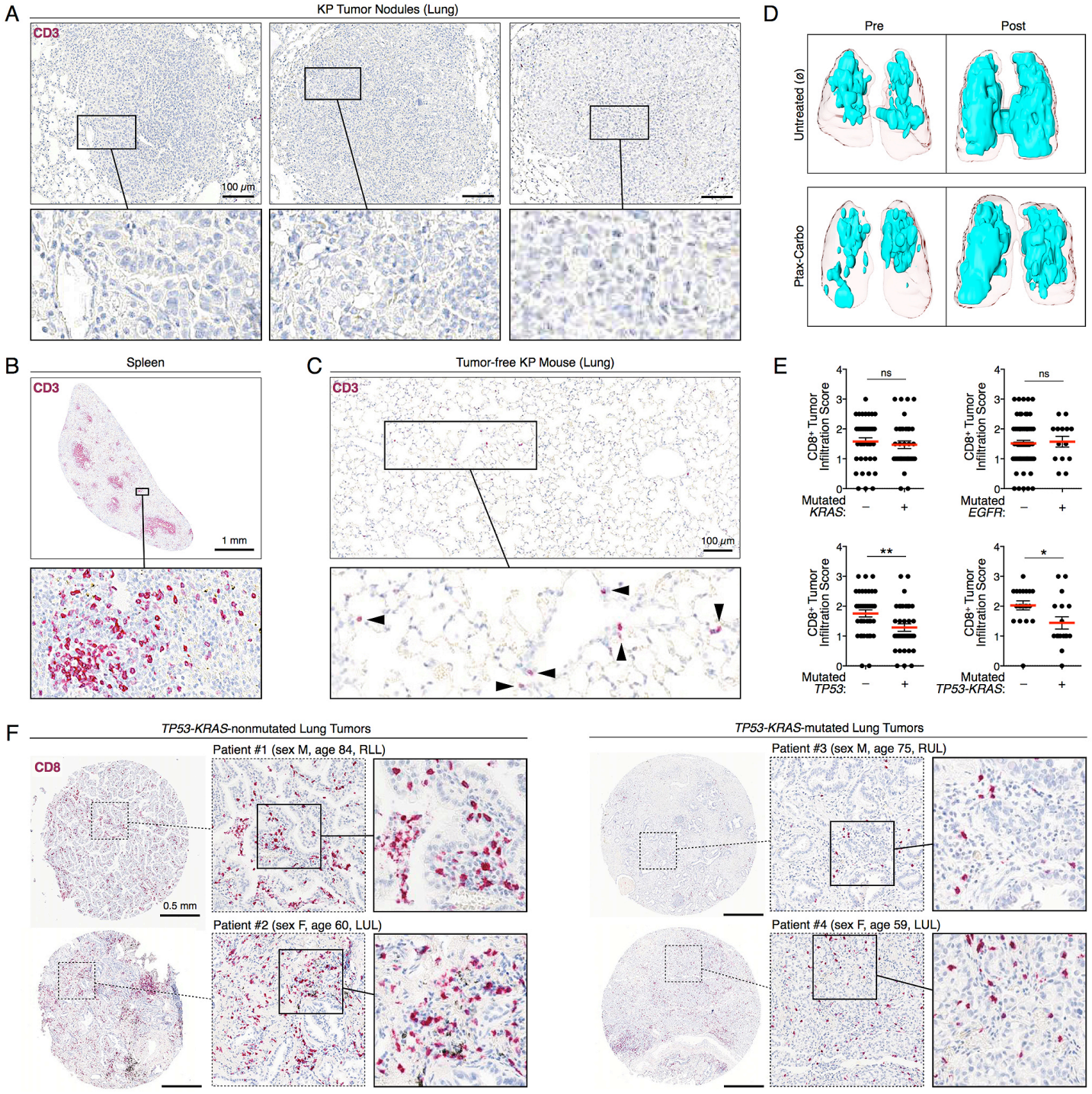

Figure S1, related to Figure 1. KP lung tumors lack infiltrating T cells, resist standard chemotherapy and reflect the human disease. (**A-C**) Immunohistochemistry (IHC) of $CD3^+$ cells (red) in KP lung tumor nodules and tumor-free lung tissue as well as spleen tissue sections as reference positive control. Arrowheads show individual stained $CD3^+$ cells. (**D**) Magnetic resonance imaging (MRI)-based detection of lung tumors in KP mice. Surface renderings of MRI images show lungs from mice that were untreated (ø, top) or exposed to paclitaxel and carboplatin (Ptax-Carbo, bottom). Color-coded images show tumors (blue) and lungs (light pink) both pre (left) - and post-treatment (right). (**E**) $CD8^+$ cell tumor tissue infiltration score, based on IHC staining (see F), in lung biopsies (n=76) from non-small cell lung cancer patients with or without *KRAS* (top, left), *EGFR* (top, right) or *TP53* (bottom, left) mutations. The bottom, right panel shows patient biopsies with *TP53-KRAS* double mutations or without *TP53* and *KRAS* mutations. (**F**) Representative IHC for $CD8^+$ cells (red) in lung tumor patient biopsies from *TP53-KRAS*-nonmutated (left) and *TP53-KRAS*-mutated (right) lung tumors. Patient identifiers are noted above each biopsy (patient #, sex, age, location of biopsy in lung (LUL, left upper lobe; RLL, right lower lobe; RUL, right upper lobe)). Scale bars as indicated.*P<0.05; **P<0.01; ns, not significant.

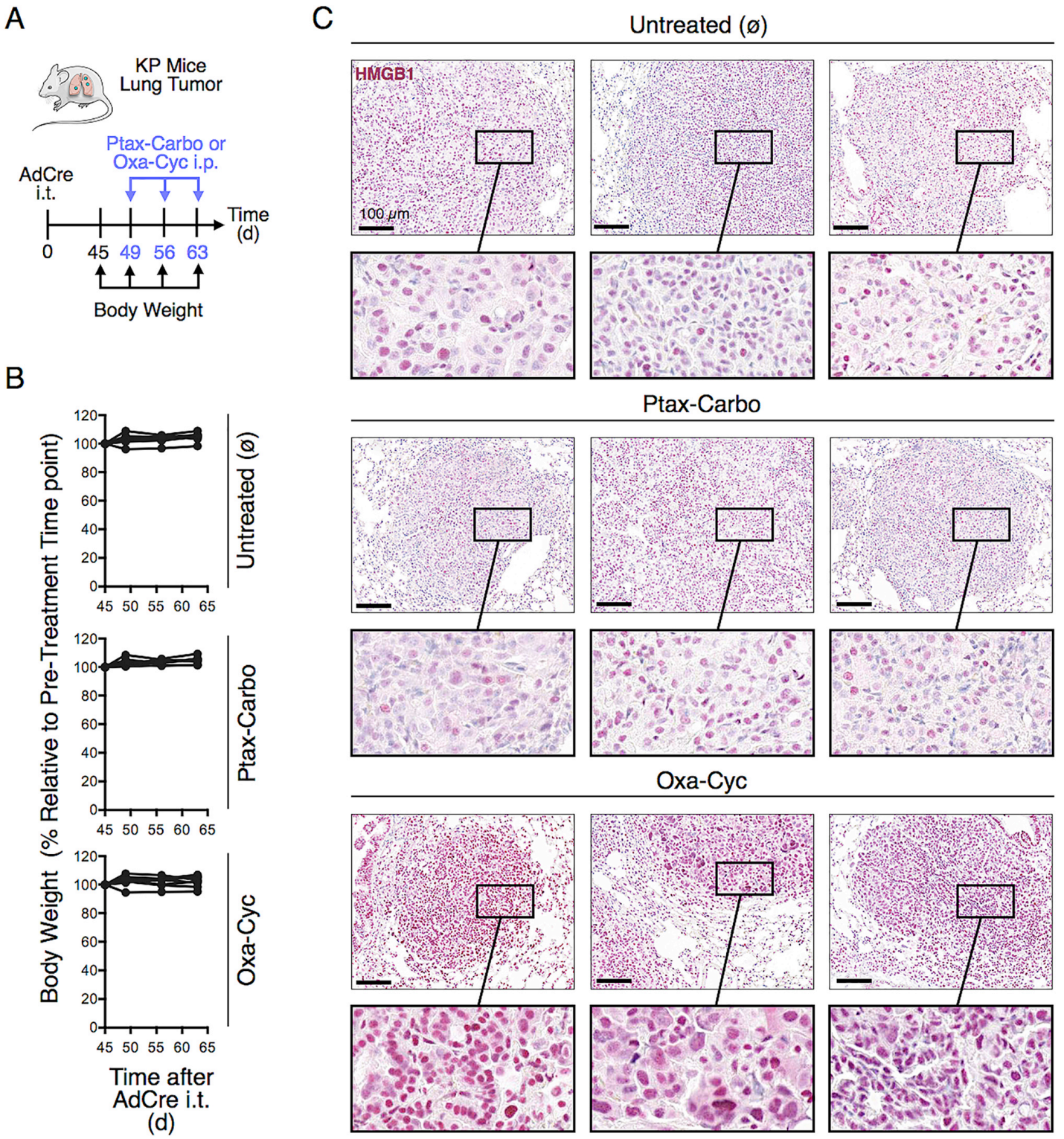

Figure S2, related to Figure 2. Oxa-Cyc chemotherapeutic drugs are well tolerated *in vivo* and increase HMGB1 nuclear staining in lung tumor cells of KP mice. (**A, B**) Experimental scheme and body weight change of drug-treated KP mice relative to a pre-treatment time point. Each line represents an individual mouse (n=7-8 mice per group) that was either left untreated (ø) or exposed to Ptax-Carbo or Oxa-Cyc. (**C**) Representative HMGB1 (red) IHC staining of KP lung tumor tissue from control mice (ø) or mice exposed to Ptax-Carbo or Oxa-Cyc (see also Figure 2D). Scale bars: 100 μm. Ptax, Paclitaxel; Carbo, Carboplatin; Oxa, Oxaliplatin; Cyc, Cyclophosphamide.

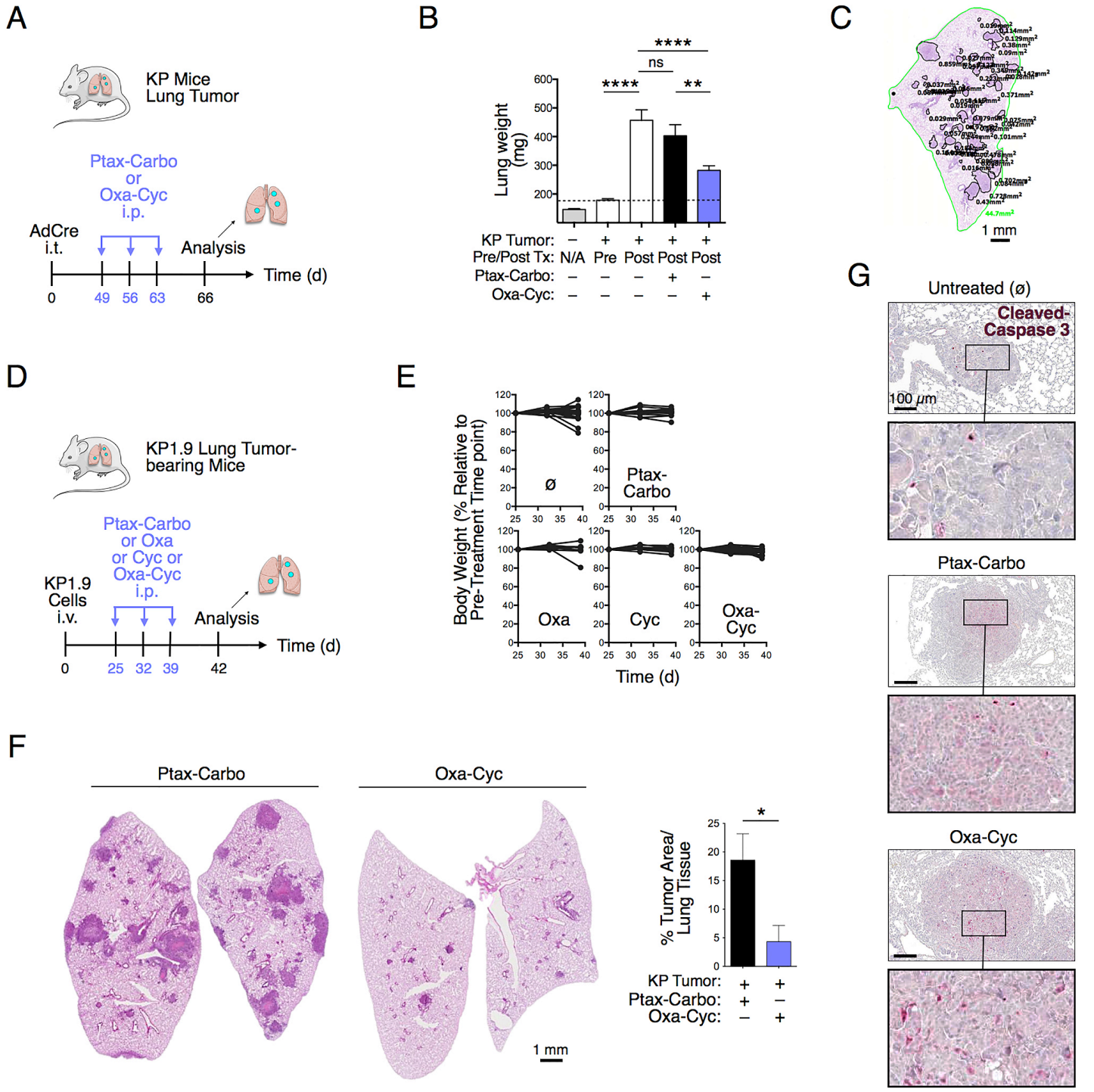

Figure S3, related to Figure 3. Oxa-Cyc suppresses lung tumor progression in KP mice and orthotopic KP1.9 tumor cell-bearing mice. (**A**) Treatment scheme of tumor-bearing KP mice exposed to either Ptax-Carbo or Oxa-Cyc. (**B**) Lung weight as proxy for tumor burden (Cortez-Retamozo et al., 2012) of mice treated as in (A). 'Pre Tx' and 'Post Tx' define pre (d45) and post (d66) treatment time points, respectively (n=10-34 mice per group). (**C**) Example of lung tumor area quantification on a hematoxylin and eosin (H&E) stained section of a KP lung tumor lobe. Encircled tumor nodules (black) and total analyzed lobe (green) areas were used to calculate % tumor area/lung tissue area. (**D**) Experimental treatment scheme of orthotopic KP1.9 tumor cell-bearing mice treated or not with Ptax-Carbo, Oxa, Cyc or Oxa-Cyc. (**E**) Body weight change of mice treated (as in D) relative to a pre-treatment time point. Each line represents a single mouse (n=8-21 mice per group). (**F**) KP1.9 lung tumor burden identification and quantification in H&E stained lung sections of mice treated (as in D) (n=3-4 mice per group). (**G**) Cleaved-caspase 3 (red) IHC in lung tumor tissue from KP mice left untreated (ø) or treated with Ptax-Carbo or Oxa-Cyc. Scale bars: 100 μm. Oxa, Oxaliplatin; Cyc, Cyclophosphamide; Ptax, Paclitaxel; Carbo, Carboplatin; **P*<0.05; ***P*<0.01; *****P*<0.0001; ns, not significant; N/A, not applicable.

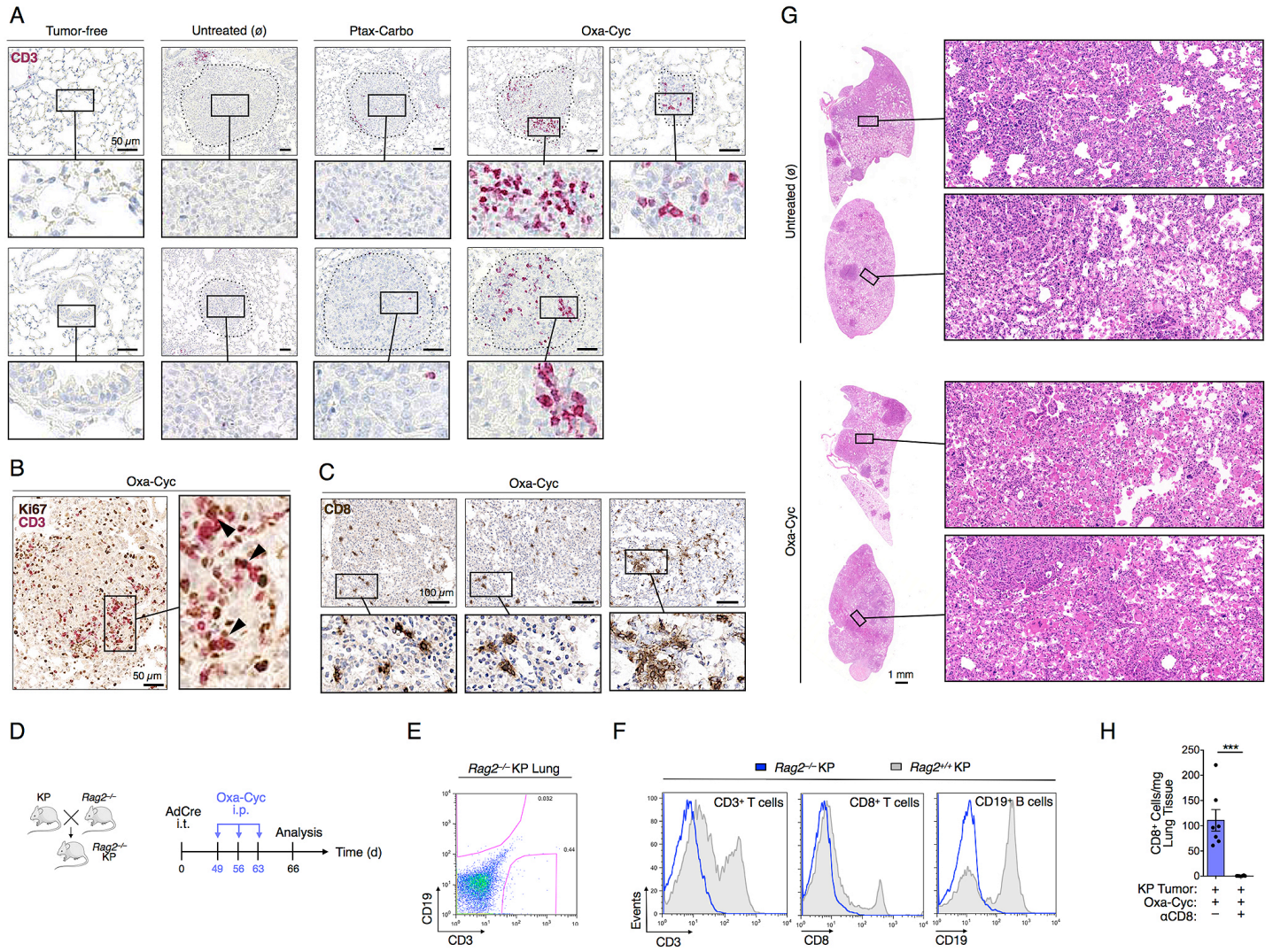

Figure S4, related to Figure 4. Oxa-Cyc instigates CD3$^+$ T cell infiltration in lung tumor nodules of KP mice and fails to suppress tumor growth in *Rag2*$^{-/-}$ KP mice. (**A**) IHC of CD3$^+$ cells (red) in tumor-free lungs, tumor tissue of untreated KP mice (ø) and tumor tissue of KP mice exposed to Ptax-Carbo or Oxa-Cyc (see also Figure 4D). Scale bars: 50 μm. (**B**) Multiple IHC showing CD3$^+$ (red) and Ki67$^+$ (brown) cells in lung tumor tissue from Oxa-Cyc-treated KP mice. Arrowheads show CD3 and Ki67 co-localization. (**C**) IHC of CD8$^+$ cells (brown) in lung tumor tissue of Oxa-Cyc-treated KP mice (see also Figure 4E). Scale bars: 100 μm. (**D-F**) Experimental approach (D) and immune profile of *Rag2*$^{-/-}$ KP mice. CD3 and CD19 flow cytometry profile (pre-gated on CD45$^+$ cells) of single cell suspensions from lungs of *Rag2*$^{-/-}$ KP mice (E). CD3, CD8 and CD19 flow cytometry profile of single cell suspensions from lungs of *Rag2*$^{-/-}$ KP mice (blue) and spleens of *Rag2*$^{+/+}$ KP mice (grey) (F). (**G**) Lung tumor identification in H&E stained tissue sections of *Rag2*$^{-/-}$ KP mice either left untreated (ø, top) or exposed to Oxa-Cyc (bottom). (**H**) Flow cytometry-based quantification of CD8$^+$ cell concentrations in lung tissue of Oxa-Cyc-treated tumor-bearing KP mice that did or did not receive anti-CD8 (αCD8) depleting mAb (n=6-7 mice per group). Oxa, Oxaliplatin; Cyc, Cyclophosphamide; Ptax, Paclitaxel; Carbo, Carboplatin; ***P<0.001; ns, not significant.

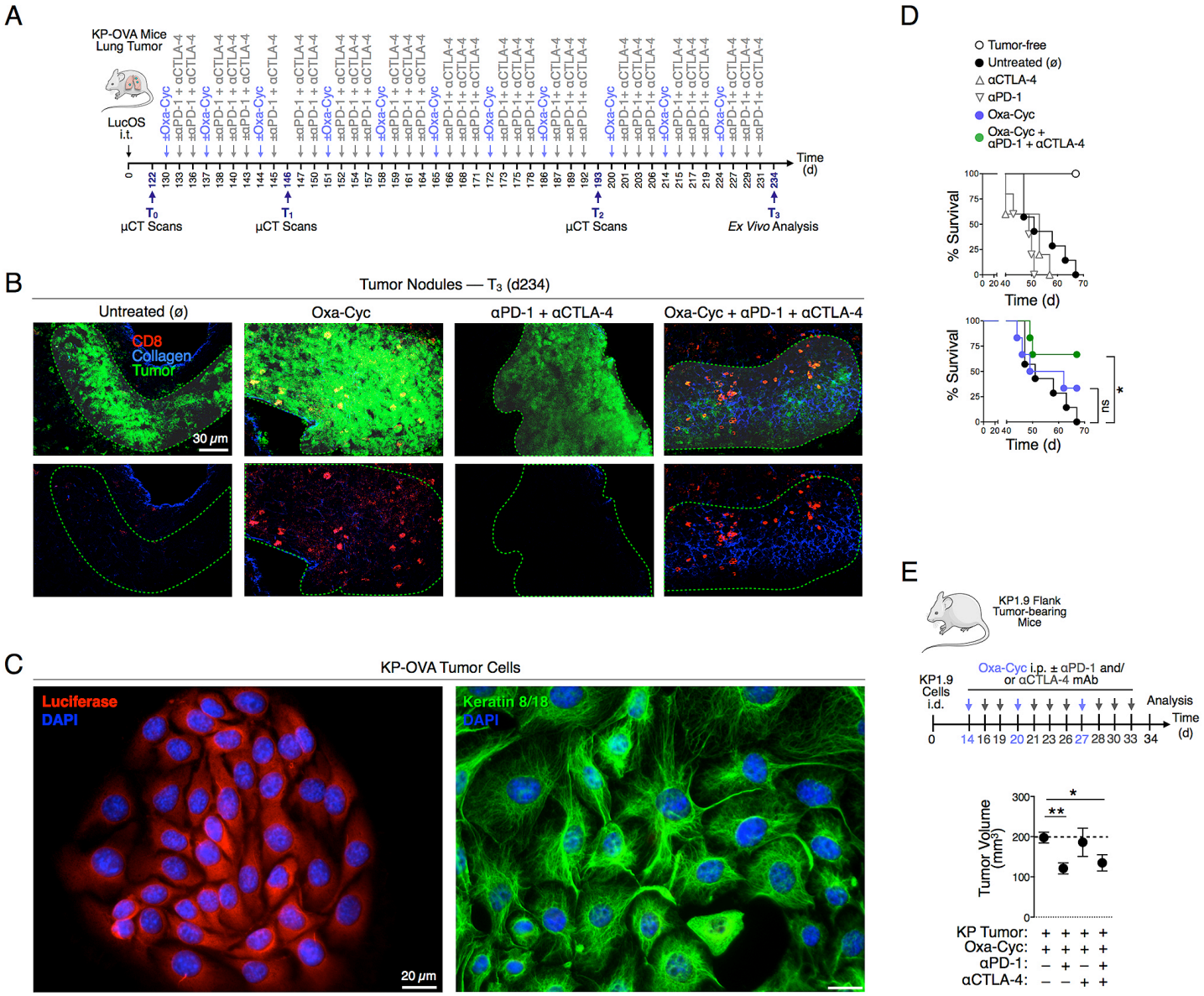

Figure S5, related to Figure 6. Oxa-Cyc fosters tumor nodule infiltration by CD8$^+$ T cells and improves tumor growth control and survival of immune checkpoint blockade-treated lung tumor-bearing mice. (**A**) Treatment scheme of a pre-clinical study in KP-OVA mice. The experimental scheme outlines when Oxa-Cyc (blue) and anti-PD-1 + anti-CTLA-4 (αPD-1 + αCTLA-4) mAbs (grey) were given to tumor-bearing KP-OVA mice. T_0, T_1, T_2 define micro-computed tomography (μCT) imaging time points whereas T_3 designates the *ex vivo* analysis time point (n=5 mice per group). (**B**) Multiphoton microscopy of CD8$^+$ cell infiltration (red) into luciferase$^+$ tumor areas (green, for visualization highlighted also by dashed green line) of lung tissue isolated from KP-OVA mice at time point T_3 left untreated (ø) or exposed to Oxa-Cyc and anti-PD-1 + anti-CTLA-4 mAbs either alone or in combination. The collagen network is shown in blue (see also Figure 6H). Scale bar: 30 μm. (**C**) *In vitro* validation of anti-luciferase Ab (red, left) used in (B) to detect luciferase-expressing tumor cells derived from KP-OVA mice. In addition, these KP-OVA tumor cells (KP-OVA-CG1 cell line) were stained with keratin 8/18 (green, right) to verify their epithelial origin. Cell nuclei (DAPI staining) are shown in blue. Scale bars: 20 μm. (**D**) Survival of tumor-free C57BL/6 mice (n=3) and of mice bearing orthotopic KP1.9 tumors, left untreated (ø) or exposed to anti-PD-1 mAbs, anti-CTLA-4 mAbs, Oxa-Cyc or combinations thereof (n=5-7 mice per group). (**E**) Oxa-Cyc improves anti-PD-1 mAb treatment in KP1.9 tumor-bearing mice. Experimental outline and tumor volume of Oxa-Cyc-treated mice also treated with anti-PD-1, anti-CTLA-4 or anti-PD-1 + anti-CTLA-4 mAbs (n=4-5 mice per group). Oxa, Oxaliplatin; Cyc, Cyclophosphamide; *P<0.05; **P<0.01; ns, not significant.

Supplemental Experimental Procedures

Mice

Kras$^{LSL\text{-}G12D/+}$;*Trp53*$^{flox/flox}$ (referred to as KP) mice were used as a conditional mouse model of non-small cell lung cancer (DuPage et al., 2009) and bred in our laboratory in the 129 background. Several experiments were replicated using KP mice in the C57BL/6 background. *Rag2*$^{-/-}$ mice (C57BL/6 background), *Tlr4*$^{-/-}$ mice (C57BL/6 background) and C57BL/6 wild type mice were obtained from the Jackson Laboratory. BALB/c wild type mice were purchased from Janvier Labs and C57BL/6 wild type mice (used for the MCA205 fibrosarcoma model) were obtained from Harlan Laboratories. All animal experiments were approved by the Massachusetts General Hospital Subcommittee on Research Animal Care, except experiments in BALB/c and MCA205-bearing C57BL/6 mice that were approved by the Ethical Committee of the Gustave Roussy Cancer Campus (Villejuif, France).

Tumor Models

To induce lung adenocarcinoma, KP mice were infected with an adenovirus expressing Cre recombinase (AdCre) by intratracheal intubation and inhalation (i.t.) or intranasal instillation (i.n.) as described previously (DuPage et al., 2009). AdCre was purchased from the University of Iowa Gene Transfer Vector Core. Treatment of i.t. infected 129 KP mice started on week 7 and of C57BL/6 KP mice on week 9 after AdCre infection, when lung adenocarcinomas are established and detectable by micro-computed tomography (μCT). Treatment of 129 KP mice infected i.n. started 12 weeks after AdCre infection. To study tumor-antigen specific T cell responses, lentiviral vectors (LucOS) containing two peptides of the ovalbumin (OVA) antigen ($OVA_{257\text{-}264}$ (CD8 epitope), $OVA_{323\text{-}339}$ (CD4 epitope)) and the SIY (SIYRYYGL) antigen fused to luciferase were used for KP mouse infection (these mice are referred to as KP-OVA mice). Lung tumors that develop in LucOS infected KP-OVA mice express the OVA and SIY antigens and luciferase as a tumor cell marker (DuPage et al., 2011). Treatment of i.t. infected 129 KP-OVA mice started 19 weeks after LucOS infection when lung tumors are established and detectable by μCT. When indicated, murine KP1.9 lung tumor cells were injected into C57BL/6 mice intravenously (i.v., $2.5x10^5$ cells in 100 μl PBS) to develop orthotopic tumors. These mice reproducibly show macroscopic lung tumor nodules at 3 weeks post tumor cell injection. Evaluation of lung tumor burden in all three models included noninvasive high-resolution μCT or magnet resonance imaging (MRI) as detailed below (see section: Micro-Computed Tomography (μCT) and Magnet Resonance Imaging (MRI)), as well as lung weight measurements and histological analyses based on hematoxylin and eosin (H&E) staining of explanted lung tissue. In selected experiments, KP1.9 tumor cells were injected intradermally (i.d., $1x10^6$ cells in 50 μl PBS) into the flank of C57BL/6 mice; tumor dimensions were measured with a digital caliper and tumor volumes defined as $\Pi/6$ x length x width^2.

CT26 colon carcinoma cells given subcutaneously (s.c., $8x10^5$ cells in 100 μl PBS) to BALB/c mice and MCA205 fibrosarcoma cells injected (s.c., $8x10^5$ cells in 100 μl PBS) into C57BL/6 mice were followed over time using caliper-based measurements; tumor sizes were calculated as length x width.

Cell Lines

The lung adenocarcinoma cell line KP1.9 was derived from lung tumors of C57BL/6 KP mice and was kindly provided by Dr. A. Zippelius, University Hospital Basel, Switzerland. The lung adenocarcinoma cell lines KP L1-3, KP L1-5 and KP L2-9 were derived from 129 KP mouse lung tumors whereas the lung adenocarcinoma cell line KP-OVA-CG1 was generated from lung tumor tissue of C57BL/6 KP-OVA mice; these cell lines were all established in our laboratory. All lung adenocarcinoma cell lines were cultured in Iscove's DMEM media supplemented with 10% fetal bovine serum (FBS) and 1% penicillin/streptomycin. The colorectal carcinoma cell line CT26, obtained from ATCC, was maintained in RPMI 1640 medium supplemented with 10% FBS, 2 mM L-glutamine, 100 IU/ml penicillin G sodium salt, 100 μg/ml streptomycin sulfate, 1 mM sodium pyruvate and 1 mM non-essential amino acids. Murine fibrosarcoma MCA205 cells were cultured in RPMI 1640 medium supplemented with 10% FBS, 2 mM L-glutamine, 100 IU/ml streptomycin sulfate, 1 mM sodium pyruvate, 1 mM non-essential amino acids and 1 mM HEPES buffer.

Human Tumor Samples

Sections from paraffin-embedded biopsies of lung resections (n=76) from non-small cell lung cancer patients with known *KRAS* and *EGFR* gene mutation status were obtained from the Department of Pathology at Massachusetts General Hospital. TP53 immunohistochemistry (IHC) was conducted with anti-p53 monoclonal antibody (mAb) clone DO-7 (Leica). *TP53* wild type or mutational status was assessed based on TP53 pattern expression as described (Köbel et al., 2010) using the following scoring system: score 0 (complete absence of staining indicates *TP53* null mutation); score 1 (focal nuclear expression in up to 50% of tumor cells presents *TP53* wild type); score 2 (nuclear overexpression in more than 50% of tumor cells represents *TP53* missense mutation). Biopsies with score 0 or score 2 were categorized as *TP53* mutants and biopsies with score 1 as *TP53* wild type. All p53-stained biopsies were reviewed in a blinded manner. CD8 IHC was performed with anti-CD8 mAb clone C8/144B (DAKO) on subsequent sections and CD8 positive cell infiltration in tumor areas scored in the following categories: score 0 (less that 5% CD8 staining); score 1 (5-15% CD8 staining); score 2 (15-25% CD8 staining); score 3 (more than 25% CD8 positive stained cells). Two independent blinded evaluations were performed and presented as mean $CD8^+$ cell tumor infiltration score.

Micro-Computed Tomography (μCT) and Magnet Resonance Imaging (MRI)

Mice infected with AdCre or LucOS plasmids were anonymized and tumor burden noninvasively evaluated through *in vivo* lung imaging at different time points (pre- and post-treatment). During the measurements, the mice were anesthetized with isoflurane gas inhalation. μCT was acquired on a Siemens' Inveon system with a 80 kVp 500 mA cone beam μCT over 360 projections and

reconstructed by modified Feldkamp cone beam reconstruction algorithm into isotropic 78 micron voxels (512 x 512 x 768 matrix). µCT tumor quantification was performed by manual segmentation in OsiriX software (The OsiriX foundation). For the µCT 3D renderings, in AMIRA software (Visage Imaging Inc), the lungs were segmented using threshold bounded region growing with a seed placed in the lung. Respiratory-gated RARE T1 weighted MRI images were acquired on a Bruker pharmascan 4.7 tesla magnet with a echo time of 14.1 ms and a repetition time of 900 ms on a 256 x 256 x 18 image matrix (voxel size of 0.215 mm x 0.156 mm x 1.0 mm). Tumor quantification of MRI images was performed by region-based thresholding of the lungs, which were manually segmented utilizing OsiriX software. The threshold was determined as the average normal lung value (n=3). Surface renderings of MRI images were done using AMIRA software. µCT and MRI tumor quantification was performed blinded to treatment groups.

Mouse Histology, Immunohistochemistry (IHC) and Immunofluorescence Microscopy

For histological analysis of tumor burden in mice, lung tissues of tumor-bearing and control animals were harvested, formaldehyde (FA)-fixed and paraffin-embedded following standard procedures. Consecutive sections were prepared and stained with H&E using the Thermo Scientific™ Shandon Varistain™ Gemini ES Automated Slide Stainer (Thermo Scientific).

For IHC, lung tissue sections were prepared and dried at 60°C for 1 h, dewaxed and rehydrated before treated with heat-induced epitope-retrieval (HIER) during which the sections were incubated in 10 mM sodium-citrate (pH6.0) or 10 mM Tris (pH9.0) buffered solutions containing 0.05% Tween heated at 120°C for 2 min. To obtain consistent and reliable staining, automated staining systems (LabVision Autostainer 360, Thermo Scientific or Leica Bond, respectively) were used. The sections were cooled down to room temperature (RT) and placed in the Autostainer. To efficiently destroy all endogenous peroxidase and alkaline phosphatase activity in the tissue, the sections were pretreated using BLOXALL endogenous enzyme blocking solution (Vector Laboratories) for 10 min. After a blocking step with normal horse or goat serum, the sections were incubated with the individual primary Abs for 1 h followed by secondary ImmPRESS polymer detection systems (Vector Laboratories) according to the manufacturers protocol. The Vulcan Fast Red Chromogen Kit 2 (red staining, Biocare Medical) and the DAB Plus Substrate System (brown staining, Thermo Scientific) were applied as substrates. Hematoxylin was used for counterstaining. Primary Abs used for IHC were: rabbit anti-CD3 (clone SP7, Abcam), rabbit anti-Ki67 (clone SP6, Abcam), rabbit anti-HMGB1 (polyclonal, Abcam), rabbit anti-cleaved-caspase 3 (polyclonal, Cell Signaling), rat anti-mouse CD4 (clone 4SM95, eBioscience). For multiple IHC, following HIER and blocking steps, the individual Abs were incubated consecutively using the chromogens indicated above. Based on the nuclear staining intensity of HMGB1 in lung tissue of KP mice with or without drug treatment, blinded scoring of stained sections was performed with the following criteria: score 0 (no HMGB1 nuclear staining); score 1 (low HMGB1 nuclear staining); score 2 (intermediate HMGB1 nuclear staining); score 3 (high HMGB1 nuclear staining).

For anti-CD8 IHC on murine lung tissue, frozen tissue sections of ~6 µm thickness were prepared using a cryostat (Leica). These sections were air-dried for at least 1 h and then fixed in acetone for 10 min at -20°C. Before incubation with Abs, the sections were rehydrated and permeabilized with PBS containing 0.2% Triton-X100 for 5 min, followed by several washes in PBS. Two primary rat anti-mouse CD8 Abs were used in parallel (clone YTS169.4, Abcam and clone 53-6.7, BD Biosciences) that both showed similar staining patterns. The NanoZoomer 2.0-RS slide scanner system (Hamamatsu) was used for image documentation.

For immunofluorescence microscopy, KP-OVA-CG1 cells were grown on coverslips, fixed in pre-cooled (-20°C) methanol for 5 min, followed by an incubation in -20°C cold acetone for 30 sec. After the cells had air dried, they were rehydrated in PBS and permeabilized using 0.2% Triton-X100 in PBS (5 min), rinsed in PBS and then incubated with the primary Abs (rabbit anti-firefly luciferase (polyclonal, Abcam) or mouse anti-keratin 8 (clone Ks 17.2, Progen) and mouse anti-keratin 18 (clone Ks 18.174, Progen)) in a wet chamber for 1 h. After three washing steps with PBS at RT for 5 min, the samples were incubated with the secondary Ab for 45 min, followed by an incubation step with DAPI (Sigma) for another 5 min. The cells were then washed twice with PBS for 5 min and once with Aqua dest. for 1 min at RT, air dried and then mounted with Fluoromount-G (Southern Biotech). Immunofluorescence microscopic images were recorded with an Axiophot microscope (Carl Zeiss). The KP-OVA-CG1 cell line was used to validate the anti-luciferase Ab as a tool to stain for luciferase expression as a marker for KP-OVA tumor cells *in situ*, used in the multiphoton microscopy approach (see section: Multiphoton Microscopy). Accordingly, KP-OVA-CG1 cells derived from lung tissue of KP-OVA mice are positive not only for luciferase as expected but also for keratin 8/18 (i.e. of epithelial origin).

Multiphoton Microscopy

Small lung pieces containing tumor-bearing and tumor-free tissue areas were carefully removed from KP lungs using scalpels. After fixation with methanol/DMSO (4:1) for 1 h at 4ºC, lung tissues were permeabilized/stained with 1% Triton-X100, 10% goat serum, FcBlock (TruStain fcX™ anti-mouse CD16/32, clone 93, BioLegend) and unconjugated anti-luciferase Ab (polyclonal, Abcam; for the specificity of this Ab to stain tumor cells in KP-OVA mice see section: Mouse Histology, Immunohistochemistry (IHC) and Immunofluorescence Microscopy) at 4ºC overnight in 500 µl of PBS, while rocking. Samples were washed twice (0.5% Triton-X100, 10% goat serum at 4ºC overnight/overday in 5 ml of PBS, rocking) and then incubated with 1% Triton-X100, 10% goat serum, FcBlock, goat anti-rabbit IgG-APC (Life Technologies) and directly conjugated Abs (CD8a-PE, clone 53-6.7, BioLegend) at 4ºC overnight in 500 µl of PBS while rocking. Before imaging, lung tissue pieces were washed twice (5 ml PBS containing 0.5% Triton-X100, 10% goat serum, at 4ºC overnight/overday, rocking). Stained lung pieces were whole mounted on a slide in a PBS filled chamber restricted by vacuum grease. A coverslip was gently pressed down on the lung tissue. Multiphoton excitation was obtained through DeepSee Ti:sapphire lasers (Newport/Spectra-Physics) tuned to 920 nm to excite PE and APC. Whole lung tissue sections were acquired by square optical sections with 15% overlap to provide image areas as large as the whole stained tissue. Emitted fluorescence was detected on an Ultima multiphoton microscope (Prairie Technologies) through 460/50 (second harmonic generation),

665/65 (APC), 595/50 (PE) band-pass filters and non-descanned detectors to generate 3-color images. The processed data shows $CD8^+$ cells (red, PE), luciferase$^+$ tumor cells (green, APC) and the collagen matrix (blue, second harmonic generation). Images were pre-processed in R statistical computing environment using RStudio and stitched/analyzed with Fiji software.

HMGB1 and Calreticulin *In Vitro* Assays

The KP L1-3, KP L1-5 and KP L2-9 tumor lines were seeded in tissue culture plates (24 well) one day before treatment with Docetaxel (Dtax, Sigma, 30 μM), Carboplatin (Carbo, Hospira, 500 μM), Oxaliplatin (Oxa, Teva, 300 μM), Mafosfamide (Maf, Sigma, 16.5, 33, 50 μg/ml) and/or Mitoxantrone (Mtx, Sigma, 4 μM) for 24 h. The cell culture plates were then centrifuged and the supernatants collected and stored at -80°C until measuring HMGB1 levels (HMGB1 ELISA Kit, IBL International GmbH). For the calreticulin assay, the cells were harvested from cell culture plates, washed with PBS and fixed with 0.25% FA for 5 min. Thereafter, the cells were washed twice with cold PBS, incubated with rabbit anti-calreticulin Ab (polyclonal, Abcam), diluted in cold blocking buffer (PBS containing 2% FBS) and incubated for 30 min on ice. The samples were then washed and incubated with anti-rabbit AlexaFluor 488 conjugated Ab (Life Technologies) in blocking buffer for 30 min on ice, followed by a final washing step. The cells were resuspended in cold PBS and investigated by flow cytometry (CyAn ADP analyzer, Beckman Coulter). Dead cells were excluded using DAPI.

***In Vivo* Drug Treatments**

KP mice, KP-OVA mice and C57BL/6 mice bearing KP1.9 lung or flank tumors were either left untreated or received chemotherapeutic drugs once a week for three weeks. The following chemotherapy was given intraperitoneally (i.p.) diluted in 100 μl PBS (or in 200 μl PBS for Paclitaxel (Ptax)): Oxa (2.5 mg/kg of body weight), Cyclophosphamide (Cyc, Sigma, 50 mg/kg of body weight), Ptax (Hospira, 10 mg/kg of body weight) and Carbo (10 mg/kg of body weight). BALB/c mice bearing CT26 flank tumors received one intratumoral injection of 50 μl PBS or chemotherapeutic drugs (Oxa (1.25 mg/kg of body weight) or Cisplatin (Sigma, 0.25 mg/kg of body weight)). MCA205 flank tumor-bearing C57BL/6 mice were treated with one intratumoral injection of 50 μl PBS or chemotherapy (Doxorubicin (Sigma, 2.9 mg/kg of body weight) or Cisplatin (0.25 mg/kg of body weight)).

Converting drug doses between species is complex and depends on a number of parameters (including species-defined drug metabolism). Nonetheless, according to FDA-guidelines on how to calculate the 'Human Equivalent Dose' from drug doses used in mice (e.g., Guidance for Industry, Estimating the Maximum Safe Starting Dose in Initial Clinical Trials for Therapeutics in Adult Healthy Volunteers, U.S. Department of Health and Human Services, Food and Drug Administration, Center for Drug Evaluation and Research (CDER), Pharmacology and Toxicology, July 2005), the drug concentrations used to treat KP mice correspond to the following in humans: Ptax 0.8 mg/kg; Carbo 0.8 mg/kg; Cyc 4 mg/kg; Oxa 0.2 mg/kg). These are within the range of the concentrations used in the clinic (Cyclophosphamide; Oxaliplatin; Carboplatin; Paclitaxel. In: UpToDate, UpToDate, Waltham, MA. (Accessed on October 27, 2015)) and are therefore unlikely to be unachievable due to toxicity. Thus the chemotherapeutic doses and schedules used in this study were not directly matched for human exposure but are within the range of the concentrations used in the clinic, after converting drug doses between species.

In indicated experiments, immune checkpoint blockade mAbs specific for PD-1 (clone 29F.1A12, 200 μg/mouse, provided by Dr. G. J. Freeman) and CTLA-4 (clone 9D9, 100 μg/mouse, BioXcell) or isotype control Ab (clone MPC-11, 100 μg/mouse, BioXcell) were applied i.p. in 100 μl PBS. MCA205-bearing C57BL/6 mice received anti-PD-1 mAbs of clone RMP1-14 (250 μg/mouse, BioXcell).

***In Vivo* $CD8^+$ Cell Depletion**

For depletion of $CD8^+$ T cells, KP mice received anti-CD8 mAb i.p. (clone 53-6.72, 200 μg/mouse, BioXcell). The Ab was diluted in PBS and injections started 3 days before the first chemotherapeutic drug injection and were continued every 2-3 days until the end of the experiment. The efficacy of CD8 T cell depletion was verified by flow cytometry.

***In Vivo* experiments with *In Vitro* Drug Pre-Treated Tumor Cells**

Where indicated, KP1.9 tumors cells were exposed to drugs before injection into mice. Specifically, KP1.9 tumor cells were incubated at 37°C for 20 h with either Oxa (300 μM) and Maf (50 μg/ml) or Ptax (100 μM) and Carbo (1000 μM) in cell culture medium (Iscove's DMEM, 10% FBS, 1% penicillin/streptomycin). Viable and dead *in vitro* drug-treated tumor cells ($5x10^5$ cells in 100 μl medium, either treated with Oxa-Maf or Ptax-Carbo) were counted using the trypan blue exclusion method. These cells were administered s.c. to the right flank of C57BL/6 mice on day -8, -4 and -2 before untreated KP1.9 tumor cells ($7x10^5$ cells in 50 μl PBS) were injected i.d. on day 0 to the ipsi- and contralateral flanks. For all of the vaccination time points, the proportion of dead *in vitro* drug-treated tumor cells was higher than 95%. In indicated experiments, mice received therapeutic in addition to prophylactic vaccinations with *in vitro* drug-treated KP1.9 cells on day 5 and 12 post KP1.9 tumor cell injection. Tumor burden of i.d. injected KP1.9 tumor cells was measured by a digital caliper and the volume was calculated $\Pi/6$ x length x width^2.

Recovery of Cells from Murine Tissues

Single cell suspensions were prepared from murine lung, spleen and bone marrow. Lungs were harvested, cut into small pieces using scissors, digested with collagenase type I (0.2 mg/ml, Worthington Biochemical Corporation) in RPMI 1640 medium for 1 h at 37°C while shaking. Where indicated, equally sized pieces of tumor stroma and corresponding tumor-free adjacent tissue were isolated

separately from lungs of Oxa-Cyc-treated or untreated tumor-bearing KP mice using surgical fine scissors. These lung tissue biopsies were transferred into 2 ml reaction tubes, cut into small pieces and digested (0.2 mg/ml, collagenase type I) in RPMI 1640 medium for 30 min at 37°C while shaking. Femurs were harvested, cleaned and the bone marrow was flushed out using a syringe containing cold flow cytometry staining buffer (PBS with 0.5% BSA and 2 mM EDTA). Digested lung tissue as well as harvested spleen and bone marrow tissues were gently meshed through a 40 μM (or 70 μM) cell strainer using a plunger. Red blood cells were removed by Ack lysis (Lonza) according to the manufacturer's instructions. The resulting single-cell suspensions were washed and resuspended in staining buffer until used for flow cytometry.

Flow Cytometry

Single cell suspensions were incubated with FcBlock (TruStain fcX™ anti-mouse CD16/32, clone 93, BioLegend) for 15 min before staining with fluorescent conjugated Abs for 45 min at 4ºC. The cells were washed with flow cytometry staining buffer (PBS, 0.5% BSA, 2 mM EDTA) and 7-aminoactinomycin D (7AAD, Sigma) was used to exclude dead cells. Doublet cells were excluded based on their forward/side scatter properties. The number of lymphocytes and myeloid cells in a given tissue was calculated based on the percentage of each cell type identified by flow cytometry (LSRII, BD Biosciences) multiplied by the total number of cells in each organ (obtained by determining viable cell numbers based on the trypan blue exclusion method). Based on cell marker expression, the following cell types were identified by flow cytometry: $CD8^+$ T cells ($CD45^+CD3^+CD8^+$), Tregs ($CD45^+CD3^+CD4^+Foxp3^+$), B cells ($CD45^+CD19^+$), lymphocyte-like cells ($CD45^+Lin^+CD11b^-$), monocytes ($CD45^+Lin^-CD11b^+Ly\text{-}6C^{hi}$), granulocytes ($CD45^+Lin^+CD11b^+Ly\text{-}6C^{int}$), $CD11b^-$ cells ($CD45^+Lin^-CD11b^-$), $CD11b^+$ cells ($CD45^+CD11b^+$), $CD11b^+CD11c^+$ cells ($CD45^+Lin^-CD11b^+Ly\text{-}6C^-CD11c^+$), $CD11b^+CD11c^-$ cells ($CD45^+Lin^-CD11b^+Ly\text{-}6C^-CD11c^-$), DC-like cells ($Lin^-CD11b^+Gr\text{-}1^-CD11c^+CD103^+$). In general, the lineage (Lin) Ab mix contained the following anti-mouse Abs, purchased from BD Biosciences: CD90.2 (clone 53-2.1), B220 (clone RA3-6B2), NK1.1 (clone PK136), CD49b (clone DX5), Ter119 (cloneTER-119) and Ly-6G (clone 1A8). The following anti-mouse Abs were used from eBioscience: Foxp3 (clone FJK-16s); from BioLegend: CD45 (clone 30-F11), CD3 (clone 145-2C11), CD8a (clone 53-6.7), CD8b (clone YTS156.7.7), CD11c (clone N418), TLR4 (clone SA15-21), CD103 (clone 2E7) and from BD Biosciences: CD4 (clone RM4-5), CD19 (clone 1D3), Ly-6C (clone AL-21), CD11b (clone M1/70), PD-1 (clone J43) and Gr-1 (clone RB6-8C5). Intracellular staining for Foxp3 was performed using the Cytofix/Cytoperm Fixation/Permeabilization Kit (BD) according to manufactures procedures. Antigen-specific T cells in lung tissue of KP-OVA mice were stained with H-2Kb/$Ova_{257\text{-}264}$ SIINFEKL tretramer (TCMetrix). Flow cytometry data were analyzed in FlowJo v.8.8.7 (Tree Star, Inc.).

Statistics

Results were expressed as mean±SEM. Statistical tests included one-way ANOVA followed by Tukey's or Dunnett's multiple comparison test. When applicable, unpaired one-tailed and two-tailed Student's t tests using Welch's correction for unequal variances were used. Comparison of survival curves was performed with the Log-rank Mantel-Cox test. *P* values of 0.05 or less were considered to denote significance (**P*<0.05; ***P*<0.01; ****P*<0.001; *****P*<0.0001; ns, not significant).

Supplemental References

Cortez-Retamozo, V., Etzrodt, M., Newton, A., Rauch, P.J., Chudnovskiy, A., Berger, C., Ryan, R.J., Iwamoto, Y., Marinelli, B., Gorbatov, R., Forghani, R., Novobrantseva, T.I., Koteliansky, V., Figueiredo, J.L., Chen, J.W., Anderson, D.G., Nahrendorf, M., Swirski, F.K., Weissleder, R., and Pittet, M.J. (2012). Origins of tumor-associated macrophages and neutrophils. Proc Natl Acad Sci U S A *109*, 2491–2496.

DuPage, M., Cheung, A.F., Mazumdar, C., Winslow, M.M., Bronson, R., Schmidt, L.M., Crowley, D., Chen, J., and Jacks, T. (2011). Endogenous T cell responses to antigens expressed in lung adenocarcinomas delay malignant tumor progression. Cancer Cell *19*, 72–85.

DuPage, M., Dooley, A.L., and Jacks, T. (2009). Conditional mouse lung cancer models using adenoviral or lentiviral delivery of Cre recombinase. Nat Protoc *4*, 1064–1072.

Köbel, M., Reuss, A., Bois, A., Kommoss, S., Kommoss, F., Gao, D., Kalloger, S.E., Huntsman, D.G., and Gilks, C.B. (2010). The biological and clinical value of p53 expression in pelvic high-grade serous carcinomas. J Pathol *222*, 191–198.